G. Legros, A. Fuentes, P. Ben-Abdallah, J. Baillargeat, P. Joulain, J.P. Vantelon and J.L.Torero, Three-Dimensional Recomposition of the Absorption Field Inside a Non-Buoyant Sooting Diffusion Flame, Opt. Lett. 30 (2005) 3311-3313.

Three-dimensional recomposition of the absorption field inside a non-buoyant sooting diffusion flame

Guillaume Legros, Andrés Fuentes, Philippe Ben-Abdallah*
Jacques Baillargeat, Pierre Joulain, Jean-Pierre Vantelon

Laboratoire de Combustion et de Détonique
1 av. C. Ader, BP 40109, 86961 Chasseneuil-Futuroscope Cedex, France

José L. Torero

University of Edinburgh
School of Engineering and Electronics, The King's Buildings, Edinburgh, EH9 3JL, UK

Compiled February 14, 2007

A remote scanning retrieval method was developed to investigate the soot layer produced by a laminar diffusion flame established over a flat plate burner in microgravity. Experiments were conducted during parabolic flights. This original application of an inverse problem leads to the three-dimensional re-composition by layers of the absorption field inside the flame. This technique provides a well defined flame length that substitutes other subjective definitions associated with emissions.

Non-intrusive methods have been widely used to better understand combustion processes. Among these methods, measurements of transmitted and/or absorbed intensities of spectral sources can be commonly found in the literature[1−2] . It is common to combine these measurements with tomography to allow obtaining spatial information of these flames. Idealized flames such as

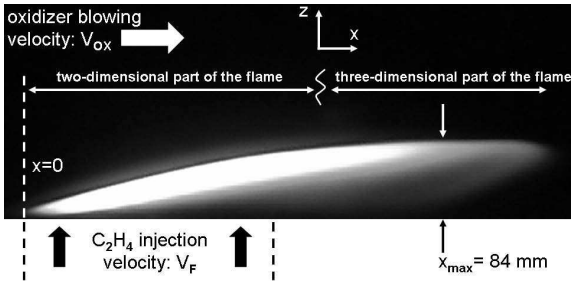

Fig. 1. Greyscale side view of the visible flame for V_{OX}=150mm.s^{-1} and V_F=3.3mm.s^{-1}.

axisymmetric jets or flat flames have been used to test numerous diagnostic techniques and their subsequent tomographic reconstructions.[1] Unfortunately, flames of practical importance exhibit, in most cases, strong three-dimensional features that make it difficult to define the pathway followed by the ray. This feature makes quantitative spatially-resolution difficult since measurements that result from integration over the line-of-sight require accurate knowledge of the characteristics of the ray pathway. A problem of fundamental physical importance is the definition of radiative fields in flames. This is especially important in diffusion flames where radiative exchange defines the characteristics of the combustion process.[1] Among the problems that require proper quantitative data, is the trailing edge quenching of a diffusion flame. Trailing edge quenching has been described as the main mechanism that defines the flame length, and thus the rate at which a fire grows. A laminar diffusion flame established inside the boundary layer formed over a flat plate in the presence of an oxidizer stream flowing parallel to the surface represents an idealized, but realistic, scenario to study quenching conditions at the trailing edge of a flame. The only complicating factor is buoyancy, thus for simplification experiments can be conducted in microgravity. The absence of buoyancy suppresses pulsations and increases the time scales associated with the combustion processes. These flames have been extensively investigated[3,4] previously, thus allowing for well characterized experimental conditions necessary for the validation of a diagnostic technique. Fig.1 shows a side view of an ethylene flame obtained by a JAI CCD camera, providing 8-bit black-and-white measurements of the visible intensity on 1280x510 pixels matrix. Close to the leading edge, the flame is mostly two-dimensional, but diffusion and convective transport in the y direction become eventually dominant. This is the region of flame quenching, thus the area where quantitative absorption measurements are necessary. These flames, albeit simple, retain the main features of interest to this study. Since the pioneer work of McCormack, numerous remote sensing methods have been developed for reconstructing physical properties of media by means of a finite number of projections. These methods require simplifications that allow the application of the reconstruction technique. Here, the assumption of a stratified medium characterized by constant physical properties at each stratum is necessary to enable the computerized tomographic reconstruction of the absorption fields at the trailing edge of the diffusion flame.

For the flame shown in Fig.1, soot is produced in the

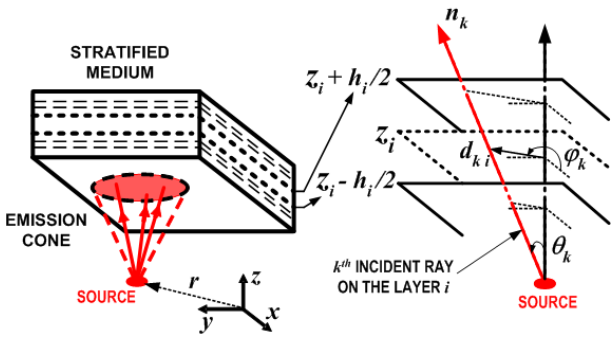

Fig. 2. Data acquisition method: media stratification on the right and k^{th} ray projection on the layer i on the left.

fuel rich region under the visible flame sheet.[2] The flame height is defined as the distance between the flame and the burner surface, and this height reaches a maximum value at x=84mm, for this particular experiment. The fuel rich region can be found between the two arrows (Fig.1) and is assumed to be stratified. The fuel rich region can then be split into a number of layers (Fig.2) of constant properties along the z direction. Thus, inside each layer, the absorption field can be considered as a two-dimensional function. In this way the spectral absorption field $G(M)$ can be expressed completely by a set of two-dimensional functions ψ_i defining the absorption field of a layer in the flame:

$$G(M) \;=\; \{\psi_i(x,y),\; z \in [z_i - \frac{h_i}{2}\,;\; z_i + \frac{h_i}{2}];\; i = 1, N\} \quad (1)$$

where z_i is the layer i centre coordinate, h_i its thickness, N the number of layers and $M(x,y,z)$ the generic point. The problem to be solved is to reconstruct the function $G(M)$ from integrated transmission measurements. For this purpose, the flame is scanned with a conic source shifted in a (x,y) plane. The source is split in a finite number of thin beams. Fig.2 shows the beam labeled k^{th} crossing the stratified layer. The fraction of the k^{th} beam absorbed in the i^{th} layer remains unknown. Measurements of the overall absorption in the k^{th} direction are made along the source scanning. With the knowledge of the measurements dependency on the source position the local absorption at each layer can then be reconstructed. In terms of geometrical optics, if $(T_{\mathbf{n}_k})$ represents the transmittance of all rays (k) propagating parallel to $\mathbf{n}_k(\theta_k, \varphi_k)$ from a source located at $\mathbf{r}$, the reconstruction problem requires to solve the following system of equations, for $k \in [1, Q]$:

$$T_{\mathbf{n}_k}(\mathbf{r}) \;=\; \sum_{i=1}^{N} \int_{-\frac{h_i}{2}}^{\frac{h_i}{2}} \psi_i(\mathbf{r} + \mathbf{d}_{ki} + s\mathbf{l}_k)\, ds \quad (2)$$

where Q is the number of beams used to split the conic source and

$$T_{\mathbf{n}_k}(\mathbf{r}) \;=\; -Log[t_{\mathbf{n}_k}(\mathbf{r})] \quad (3)$$

$$\mathbf{d}_{ki} \;=\; (z_i\, tg\theta_k\, cos\varphi_k\;,\; z_i\, tg\theta_k\, sin\varphi_k) \quad (4)$$

$$\mathbf{l}_k \;=\; (tg\theta_k\, cos\varphi_k\;,\; tg\theta_k\, sin\varphi_k) \quad (5)$$

This strongly non-linear problem can be considerably simplified by applying a two-dimensional Fourier transformation to Eq.(2), which leads to the following equation for any k:

$$\hat{T}_{\mathbf{n}_k}(\mathbf{w}) \;=\; \sum_{i=1}^{N} \int_{\mathbb{R}^2} \frac{\int_{-\frac{h_i}{2}}^{\frac{h_i}{2}} \psi_i(\mathbf{r} + \mathbf{d}_{ki} + s\mathbf{l}_k)\, ds}{e^{2\pi <\mathbf{r},\mathbf{w}>}}\, d\mathbf{r} \quad (6)$$

where $\mathbb{R}$ represents the real numbers, $\mathbf{w}$ represents the two-dimensional Fourier vector. This transformation is possible as soon as the source is shifted in a (x,y) plane to define a dependency of $T_{\mathbf{n}_k}$ on x and y. The integral operators can then be switched and using the Fourier transform property, the system to be solved can be reduced to the following expression valid for any k:

$$\sum_{i=1}^{N} \frac{sin\,(\pi h_i < \mathbf{l}_k, \mathbf{w} >)}{e^{-2j\pi <\mathbf{d}_{ki}, \mathbf{w}>}\, \pi \;< \mathbf{l}_k, \mathbf{w} >}\, \hat{\psi}_i(\mathbf{w}) \;= \hat{T}_{\mathbf{n}_k}(\mathbf{w}) \quad (7)$$

Thus, the left member of Eq.(7) appears as the product of two matrices. The dimension of the first matrix is QxN and its terms only depend on the geometrical characteristics of the Q rays and the chosen media stratification. The second matrix is the Nx1 vector of the unknown $\hat{\psi}_i(\mathbf{w})$ (i=1,N) at a location $\mathbf{w}$ in the Fourier space. The right member of Eq.(7) represents the Qx1 vector of the transformed measured transmittances $\hat{T}_{\mathbf{n}_k}(\mathbf{w})$ (k=1,Q) at the same location $\mathbf{w}$.

The procedure to solve this inverse problem starts with a Fast Fourier Transformation (FFT) of the transmittances whose dependencies on x and y are given by the measurements at the P_xxP_y positions of the source in the plane (x,y), providing P_xxP_y vectors $\hat{T}_{\mathbf{n}_k}(\mathbf{w})$ (k=1,Q). The system to be inversed consists in P_xxP_y Eq.(7). As this system is *a priori* ill-defined, its solution requires iterations using the Tikhonov regularization method.[6] Eventually, the vectors $\hat{\psi}_i(\mathbf{w})$ (i=1,N) are computed at P_xxP_y locations in the Fourier space and an inverse FFT provides the sought $\psi_i(\mathbf{r})$ (i=1,N) at the P_xxP_y source locations in the (x,y) plane. This means that the spatial resolution of the technique corresponds to the distance between two source positions and could be optimized, what was not this study goal.

The overall procedure was checked with a theoretical stratified media where the absorption field depends linearly on the three coordinates. The algorithm does not allow constraining boundary conditions to physically possible values therefore the first iteration requires a realistic field. It was observed that if the first iteration starts with realistic absorption fields, the inversion converges quickly and computes the layer absorption fields with excellent agreement.

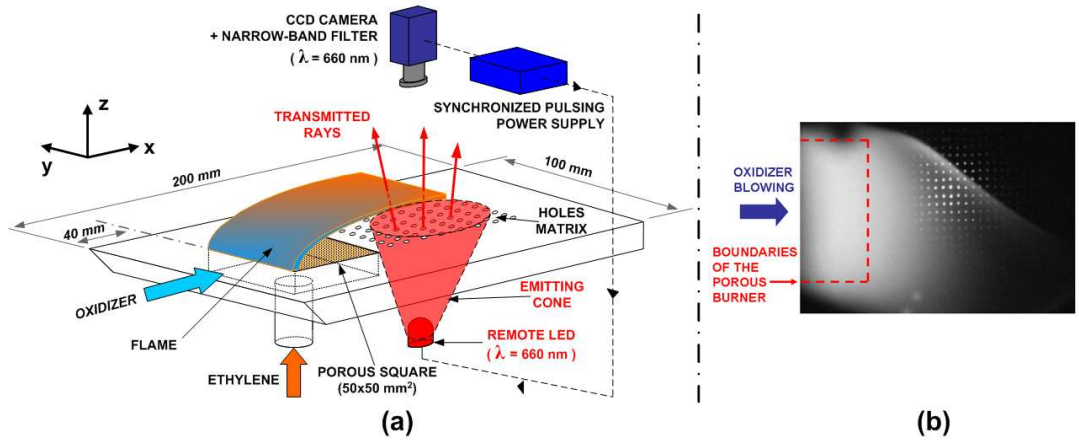

Fig. 3. (a) Experimental setup and (b) Frame recorded when the LED is on (same conditions as for Fig.1).

The experimental application of this procedure for the microgravity flame needed to comply with several requirements. First of all, as far as possible, the radiative characteristics of the burner plate should remain unchanged. For this reason, the holes through which the light was introduced were constrained to small 1.4mm-diameter perforations. Fig.3(a) shows the matrix consisting of 21x18 holes used. The distance between contiguous holes was 2.8mm and a Pyrex glass plate was placed underneath the holes to prevent the flow of oxidizer through them. A 60mW LED provides the emitting cone at λ=660nm. This cone crossed the plate with the holes to produce the beams. In the wavelength region around λ=660nm, absorption within diffusion flames is mainly due to soot.[1] This choice of wavelength eliminates gas phase absorption. Furthermore, the CCD of the 8-bit progressive scan monochrome JAI camera exhibits good linearity and sensitivity in this wavelength. The camera was mounted with a narrow band filter centred at λ=660nm and with a band width at one half the transmissivity maximum of 20nm. Transmitted light was measured at 50Hz on a matrix of 640x494 pixels (Fig.3(b)). The camera spatial resolution of approximately 0.2mm is therefore far higher than the technique resolution. The emission from the flame needs to be subtracted, thus the LED was pulsed and measurements were made when the LED was on and off. The measurements were then subtracted. Baseline measurements were made without a flame to be able to calculate the transmittances. The LED was shifted in a (x, y) plane located 50mm under the burner surface. The flame was established on board the Novespace Airbus Zero-G, providing 22s of microgravity. More details about the experimental environment can be found in Ref.2. Steady-state was reached after 5s, therefore, the available microgravity duration is of 17s. This limited the quickest scanning to 8x8 positions of the LED. For each position, a square set of 9x9 holes was found to be bright and homogeneous enough to enable relevant transmittance measurements.

The frames post-processing provides the required overall transmittances of the 81 rays generated by a 9x9 hole square matrix at each of the 64 source positions distributed in a 8x8 square matrix. Images like Fig.1 define z=30mm as a reasonable height for the domain to be investigated. Beyond 30 mm absorption tends towards zero at this height. The domain was then stratified into 60 layers along the z-axis, giving a layer height of 0.5mm. The sensitivity of the inverse processing was found to be small for this layer thickness. The realistic absorption profile necessary for the first iteration was obtained by conducting transmission measurements along the z-axis at x=55mm.[2] These measurements are only accurate when conducted within the two-dimensional region of the flame, thus the choice of location. This profile was then used to initialize the vectors $\hat{\psi}_i(\mathbf{w})$ (i=1,N) at (0,0) of the Fourier space. Fig.4(a) shows the computed absorption field in the layer located at z=14.5mm. This absorption field resembles well the expected distributions of soot computed in a previous study for these flames.[7] It is important to note the three-dimensionality of the absorption field.

Fig.4(b) shows the absorption profiles at the symmetry plane of the burner. The arrow indicates the location of the flame. It can be observed that the peak absorption values increase slightly up to x_{max} for $x = 85.4mm$. The maximum absorption seems to coincide with the locus of the maximum flame height (x_{max}) within the constraints of the model accuracy, i.e. 2.8 mm. This continuous increase in the absorption peak indicates that soot formation is greater than soot oxidation. Beyond x_{max} the maximum absorption value decreases slowly indicating that oxidation is being favoured over soot production. These general observations are in agreement with those reported for microgravity axisymmetric flames.[1] The relative location of the visible flame with respect to the absorption peak also changes as x_{max} is crossed. For $x \leq x_{max}$, the visible flame remains in an area where

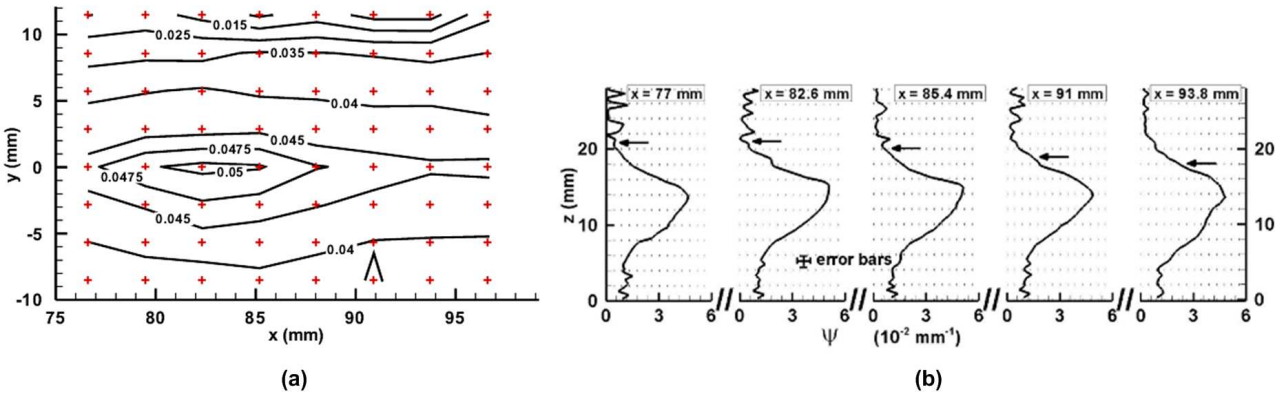

Fig. 4. (a) Absorption field (in mm^{-1}) in the layer located at z=14.5mm. The crows betrays the source positions and (b) Absorption profiles at y=0. The arrows indicates the visible flame height.

there is little soot and corresponds mostly to complete oxidation of the fuel and thus is characterized by strong CH^* radicals emissions. Earlier measurements of CH^* radicals validate this observation.[2] The height (z) of the peak increases with x in this region. For $x \geq x_{max}$, the visible flame location moves towards the peak absorption with x while the absorption peak decreases in height (z). The visible flame corresponds mostly to soot oxidation and the emissions of CH^* have been found to decrease towards eventual extinction.[2] For this kind of "Open-Tip" flame (i.e. releasing hot soot through the trailing edge), emissions follow decay functions, thus the exact location for the final quenching of the flame and its relationship to visible emissions is difficult to define and always requires the definition of an arbitrary threshold. This novel diagnostic technique provides quantitative evidence in support of using x_{max} as a characteristic flame length.

*Present address, Laboratoire de Thermocinétique de Nantes Rue C. Pauc, BP 90604, 44306 Nantes Cedex 3, France

References

1. C.M. Megaridis, B. Konsur and D.W. Griffin, "Soot-Field Structure in Laminar Soot-Emitting Microgravity Non-Premixed Flames," *Proc. Combust. Inst.* **26,** pp. 1291-1299 (1996).
2. G. Legros, P. Joulain, J.P. Vantelon, A. Fuentes, and J.L. Torero, "Soot Volume Fraction Measurements in a Three-Dimensional Laminar Diffusion Flame Established in Microgravity," accepted for publication in *Combust. Sci. Technol.* (2005).
3. T. Vietoris, J.L. Ellzey, P. Joulain, S.N. Mehta and J.L. Torero, "Laminar Diffusion Flame in Microgravity: the results of the Mini-Texus 6 Sounding Rocket Experiment," *Proc. Combust. Inst.* **28,** pp.2883–2889 (2000).
4. L. Brahmi, T. Vietoris, P. Joulain and J.L. Torero, "Détermination par Caméra Infrarouge des Distributions de Température sur l'Enveloppe d'une Flamme de Diffusion Etablie sur un Brûleur Plat en Microgravité," *Entropie* **215,** pp.69–73 (1998).
5. A.M. MacCormack, "Representation of a fonction by its line integrals, with some radiological application I, II," *Applied Phys.* **35,** pp.2908–2912 (1964).
6. P. Ben-Abdallah, "A variational method to inverse the radiative transfer equation: application to thermal sounding of atmospheres of giant planets," *J. Quant. Spect. and Rad. Trans.* **60,** pp.9–15 (1998).
7. S. Rouvreau, P. Joulain, H.Y. Wang, P. Cordeiro and J.L. Torero, "Numerical Evaluation of Boundary Layer Assumptions Used for the Prediction of the Stand-Off Distance of a Laminar Diffusion Flame," *Proc. Combust. Inst.* **29,** pp. 2527–2534 (2002).